

SIXTH EUROPEAN ROTORCRAFT AND POWERED LIFT AIRCRAFT FORUM

Paper No. 25

EXPERIMENTAL AND ANALYTICAL STUDIES OF A
MODEL HELICOPTER ROTOR IN HOVER

F. X. Caradonna and C. Tung

Aeromechanics Laboratory
U.S. Army Research and Technology Laboratories (AVRADCOM)
Moffett Field, California 94035 U.S.A.

September 16-19, 1980
Bristol, England

THE UNIVERSITY, BRISTOL, BS8, 1HR, ENGLAND

EXPERIMENTAL AND ANALYTICAL STUDIES OF A
MODEL HELICOPTER ROTOR IN HOVER

F. X. Caradonna
C. Tung

Aeromechanics Laboratory
U.S. Army Research and Technology Laboratories (AVRADCOM)
Moffett Field, California 94035 U.S.A.

ABSTRACT

The present study is a benchmark test to aid the development of various rotor performance codes. The study involves simultaneous blade pressure measurements and tip vortex surveys. Measurements were made for a wide range of tip Mach numbers including the transonic flow regime. The measured tip vortex strength and geometry permit effective blade loading predictions when used as input to a prescribed wake lifting surface code. It is also shown that with proper inflow and boundary layer modeling, the supercritical flow regime can be accurately predicted.

LIST OF SYMBOLS

A = ratio of vortex circulation to maximum blade-bound circulation
AR = aspect ratio
 C_l = sectional lift coefficient
d = radial distance from a vortex to a flow-field point
R = radius of the rotor blade
r = radial distance from the rotor center of rotation
 V_i = vortex-induced velocity
 V_R = residual velocity in the wake
y = r/R, nondimensional radial coordinate
z = axial distance from rotor
 Ω = rotational speed
 Ψ = azimuthal angle measured from the point of blade overhead passage
 Ψ_v = vortex age, the azimuth angle, Ψ , when vortex strikes the probe

1. Introduction

The past two decades have seen a continuing development of methods to predict rotor hover performance with increasing accuracy. These methods include lifting line [1,2,3], lifting surface [4,5,6], and finite difference [7] methods. Practically speaking, none of these methods is self-contained; they all require the specification of empirically obtained wake data (strength and geometry) in order to have a correct downwash distribution. Inevitably, the development of these codes becomes a tuning process in which it is determined just how detailed and accurate a wake description must be. This stage of code development places great reliance on the available body of experimental rotor data.

The available rotor data include a sizeable number of tests where detailed blade loading is obtained using surface pressure transducers [8,9,10,11], and more recently by laser doppler velocimetry [12,13]. There is also a number of tests in which the rotor wake geometry is defined by flow visualization techniques [5,14] for a wide variety of blade configurations. Of the various wake studies, only Boatwright [15] and Cook [16] made detailed investigations of the wake flow structures. Cook's work is especially significant in that he was able to measure the strength of the tip vortex by a curve-fitting technique using hot-wire data. However, there seem to be no useable data in the literature in which simultaneous blade load distribution and wake measurements are made.

It is the intention of the present study to help fill this gap in the literature. This paper will describe the experimental set-up in which steady blade pressures were obtained using hub-mounted transducers and tip vortices were measured using Cook's technique. The data obtained are for unstalled flow ranging from the low subsonic to transonic conditions. It is shown herein (using Summa's lifting surface code [6]) that the blade-loading distribution could not have been predicted using only the classical vortex data of Landgrebe [14] and Kocurek [5].

2. The Experiment

The data presented in this paper were gathered in the Army Aeromechanics Laboratory's hover test facility, a large chamber with special ducting designed to eliminate room recirculation. The rotor, situated in the center of the chamber, was mounted on a tall column containing the drive shaft (Fig. 1). The rotor employed two cantilever-mounted, manually adjustable blades. These blades used an NACA 0012 profile and were untwisted and untapered. An aspect ratio of 6 was chosen in order to maximize Reynolds Number and available instrumentation space. The blades were grooved to accommodate 60 pressure tubes each. These tubes connect to a special cluster of three 48S8 Scanivalves (using Statham PA 856-15 transducers) driven by one SS5-48 solenoid drive mounted in the rotor hub. This arrangement permits an ample number of ports for five measurement locations - three radial locations on each blade, with one location being identical on both blades for comparison purposes. The Scanivalve stepper motor was actuated by a digital data system which acquired the data, computed the centrifugal pressure drops, and displayed the final pressure distribution. The resulting pressure distributions for collective pitch settings of 5°, 8°, and 12° are shown in Figs. 2, 3, and 4. It is seen here that the inboard pressure distributions are only slightly affected by rotor speed. However, the outboard sections show considerable pressure alteration and shock development as the tip Mach number approaches near sonic values. Overall, however, the spanwise load distribution (obtained by pressure integration) is remarkably little affected by tip Mach number (Fig. 5).

Wake data were acquired with a traverse-mounted DISA 55P01 hot-wire probe mounted beneath the rotor. Data from the wire are acquired at various points along the tip vortex trajectories and can give both the tip vortex geometry and strength. One problem with this approach is that the vortex trajectory is not steady and the probe location (which is chosen by an on-the-spot decision as to where the number of vortex core "hits" is maximized) contains some as yet undetermined error. The resulting data stream has considerable variability. However, in order to be certain of the vortex location, the only acceptable data are those where the vortex core actually hits the probe. In the digitization process (done off-line at a reduced tape speed), the above-mentioned data system was coded to look for and accept only those data which showed the

characteristic signal dip which indicates a probe-vortex strike. This turns out to be a very small percentage of the total amount of data actually recorded. A typical hot-wire trace displaying the above-mentioned variability is shown in Fig. 6.

3. Hot Wire Data Analysis

The idea of the current data analysis is that a tip vortex should look like an infinite line vortex to a sufficiently close probe. Unfortunately, the probe measures not only the velocity induced by the vortex at hand, V_i , but also that induced by the blade and the remainder of the wake system as well, V_R . The problem in analyzing the probe data is, then, how to separate this residual velocity, V_R , from the immediate vortex-induced velocity, V_i . Cook [16] handled this problem by assuming that the residual velocity was constant and given by the translation velocity of the tip vortex. He then was able to find the vortex strength by a fitting process. This strength was found to be far less than the computed maximum blade bound circulation of the single, full-scale blade used in that test. It was also found that the vortices measured were distinctly non-classical in that they contained a large rotational region outside of the viscous core. In what follows, we shall use a process very similar to Cook's in analyzing wake data.

First consideration is given to the vortex trajectories. Figure 7 shows the axial and radial components of the vortex trajectories for a pitch setting of 8° . This figure gives data for a wide range of rotor speeds, and it is apparent that the trajectory is essentially independent of tip speed — even into the transonic regime. Figure 7 together with Fig. 5 suggests that the nonlinear transonic flow on the blade has little effect on the far-field induced flow as long as the local lift is not greatly altered. Also plotted on this figure is the vortex trajectory given by Kocurek's wake-fitting formula for rotors in free air. Although the axial component of the trajectory compares well with Kocurek's formula, there appears to be a greater discrepancy in the contraction than can be explained by measurement error. The vortex trajectories for pitch settings ranging from 5° to 12° are given in Fig. 8.

The present aim in analyzing the rotor wake is only to find the vortex strength and not a complete description of the structure. This strength will be found by fitting the wake data to the velocities obtained from an appropriate combination of inviscid, two-dimensional vortices. The velocity from one such vortex is given by

$$\frac{V_i}{\Omega R} = A \frac{(C_{\ell} y)_{\max}}{4\pi AR} \frac{1}{d/R} \quad (1)$$

where the strength of the vortex is described by A , the ratio of the vortex circulation to the maximum bound circulation of the blade (determined from the pressure data). To accomplish this fitting, it is first necessary to convert the spatially dependent Equation (1), into a time-dependent expression, as the vortex data are time-based. Assuming that A is constant (which seems to be true within reasonable error bounds), the conversion to a time-dependent function is accomplished by expressing d as a function of time using the vortex trajectory data of Fig. 8. The next step is the determination of the residual velocity, V_R , which must be vectorially added to V_i before a comparison can be made with the probe data. We have done this in two different ways:

1) The first way to determine V_R involves very young vortices (about 50° old). For these it was assumed that V_R was given by the vortex trajectories (Fig. 8). The fitting process always commenced when the vortex core hit the

probe and ended when the following blade passed over; this assured the simplest possible flow field, as there would be vortices on only one side of the probe and minimal influence of vortex sheets and blade bound vorticity. Figure 9 shows some typical comparisons of probe data with the fitting expression. This figure shows the vortex velocity-time traces for pitch settings of 8° and 12° . It is seen here that the fitting curve provides a good match to the data outside of the immediate core region. Furthermore, the vortex strength is very close to the maximum blade bound circulation.

2) A second means to determine V_R was required in analyzing older vortices (about 210° old). The flow is more complex in this case, as the probe always lies between two vortices in the fitting region, and the expression for the vortex-induced velocity is correspondingly complicated. In fact, V_i , for this case was determined using three vortices - one outboard of the probe and two inboard. Again, the data were fit for the time period between a probe-vortex strike and the subsequent blade passage. It was found that with V_R determined by the vortex trajectory data, it was not possible to obtain a good fit of the classical vortex expression to the wake data. Instead we found that a better value for V_R was found by use of the minimum measured velocity between two vortices. At this point, the vortex-induced velocity is small, but not zero (due to the differing instantaneous translation velocities of the three vortices). The minimal induced velocity is calculated (assuming some value of A) and subtracted from the minimum measured inter-vortex velocity to obtain V_R . This task was rendered quite simple by the fact that the radial component of these velocities turns out to be very small (this was checked by calculations and measurements with a second probe). Since the two methods above do not give the same value for the residual velocity, it is clear that V_R is not a constant in this case. We assume, however, that it changes sufficiently slowly to render the fitting process meaningful. In fact, the results thus obtained are consistent with the young vortex data. Figure 10 shows some typical comparisons of the older vortex data with the fitting expressions. This figure shows the fittings for pitch settings of 5° , 8° , and 12° . It is seen that the 8° and 12° cases show vortex strengths which match the maximum blade-bound vorticity very well. At 5° pitch, however, the strength is seen to be considerably smaller.

It seems from the above data, which are taken at a low rotor speed, that the tip vortex develops its full strength very early in life (mainly before 50°). Although there is a fair amount of variability between vortices, it is rather striking that very many vortices closely approach a classical Rankine vortex in appearance. Furthermore, the vortices (except for the 5° case) seem to contain all of the blade circulation. This vortex strength and structure differs markedly from the result obtained by Cook and probably reflects the considerable differences in blade geometries. As rotor tip speed increases (Fig. 11), however, there appears to be an increasing departure from the Rankine vortex appearance. Nevertheless, the nondimensional vortex strength seems unaffected by tip speed.

4. Comparison of Theory and Experiment

In order to integrate the present wake and loading data into a believable whole, it is necessary to be able to reproduce the blade loading computationally. We have chosen to do this using A.M.I.'s lifting surface code [6]. This is a very flexible, compressible, lifting surface code which can handle either prescribed or free wakes.

Initial efforts to compute the blade loading were done using the Kocurek wake geometry [5]. The resulting computed thrust coefficient was too high by about 20%. The next step was to compute the loading using the measured vortex locations and strength. Figure 12 shows a comparison of the measured and computed loading using the measured vortex parameters for a collective pitch of 8° (the trajectory is given by Fig. 8 and we choose $A = 1.0$). The comparison is now considerably improved and the thrust coefficient is over-predicted by less than 5%. In view of the previously mentioned uncertainties in the vortex trajectory measurements, these computations were also performed with the entire vortex trajectory perturbed such that at $\psi = 180^\circ$, the axial and radial perturbations were $\pm 0.025R$. The results derived from all possible combinations of these axial and radial changes fill the shaded area in Fig. 12. That the above measured and computed results are roughly centered on this shaded region indicates that for this case the measured trajectories are fairly accurate. However, the best comparison with the measured loading occurs when the vortex radial location (at $\psi = 180^\circ$) is increased (that is, the contraction is decreased) by $0.025R$. The identical situation was found to occur in computations of the 12° pitch cases; i.e., the best comparison occurred when the radial vortex location was increased by $0.025R$ over the measured value (Fig. 13). For the 5° collective-pitch case, the situation was a little different in that a reasonable comparison of computation and loading data could not be made until the vortex strength was reduced to $A = 0.75$. In this case, the vorticity which would otherwise have been in the tip vortex was now included in the vortex sheet model. (For a complete description of the assumed vortex sheet model see Ref. [6]). This result is consistent with the measured vortex strength and gives the comparison shown in Fig. 14.

The previous comparisons have been made at low tip Mach numbers. The lifting surface code used should be applicable to predict the spanwise and chordwise loading up to the onset of supercritical flow. Beyond this point, linear aerodynamics are not applicable on the blade and a more complete flow description is required. As a preliminary evaluation of the high-speed flow data, two-dimensional computations were made of the flow at the 80% radial station. This was done using Holst's full-potential code [17]. In order to perform this computation, an angle of attack is required. Since the region of supersonic flow is localized (i.e., limited to the immediate vicinity of the upper blade surface), it should be possible to find the angle of attack using the linear lifting surface code. Of course, the lifting surface code requires the measured vortex location and strength as mentioned previously. With the angle of attack obtained thereby, the Holst code produced the results shown in Fig. 15. This figure shows two computed results — an inviscid result and one with a viscous ramp-boundary layer model [18]. It is seen that a shock-boundary layer interaction model is very necessary and in this case very effective.

5. Concluding Remarks

The present study was intended as a benchmark to aid in the development of hover performance codes. The goal was to obtain simultaneous measurements of blade load distribution and tip vortex geometry and strength using fairly standard techniques. In spite of some uncertainties (due mainly to wake unsteadiness), lifting surface computations show that the load and wake measurements are generally consistent with each other.

The main conclusions from this study are:

1. The Cook vortex measurement technique seems to be quite effective for two-bladed rotors.

2. At low rotor speeds, an untwisted, untapered, double-bladed rotor produces tip vortices which can closely resemble a classical Rankine vortex. Except for the lowest pitch settings, this vortex strength closely approaches the maximum blade bound circulation. At higher tip speeds, the inner vortex structure appears increasingly nonclassical; however, the strength is unaltered.

3. It is not possible to predict the blade-spanwise-load distribution without accurate vortex location and strength data. The present measured vortex location data were significantly different (for presently unknown reasons) from the classical data in the literature. However, these measurements were indispensable to obtaining a reasonable comparison of theory and experiment.

4. For the present rotor and speed range tested, the onset of transonic flow was found to have no effect on the spanwise loading distribution and the vortex trajectories. The chordwise loading is profoundly altered by the transonic flow and can only be simulated by nonlinear aerodynamic techniques which employ a shock-boundary layer interaction model.

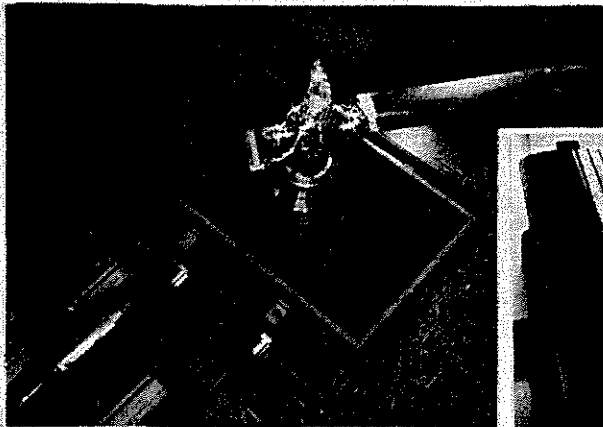
ACKNOWLEDGMENTS

This work represents the contributions of many excellent people. We would like to extend our thanks to W. D. Vann (Ft. Eustis Directorate, U.S. Army Applied Technology Lab) and H. Jones (U. S. Army Research and Technology Labs) who were instrumental in initiating our computational studies. Special acknowledgment is due to Georgene Laub who tirelessly and ably assisted in the running of the test. Thanks also to M. Summa (Applied Mechanics Inc.) who wrote the lifting surface code and assisted us in running it; S. C. Lee (University of Missouri) and T. L. Holst (NASA Research Center) who provided us with the finite difference computations.

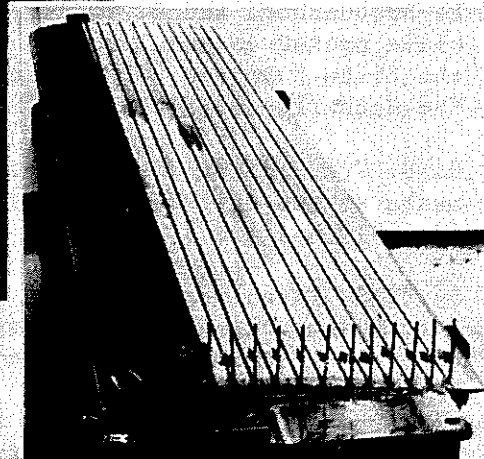
REFERENCES

1. P. Crimi, Theoretical prediction of the flow in the wake of a hovering rotor, CAL Report No. BB-1994-S-1 and No. BB-1994-S-2, Cornell Aeronautical Laboratory, Inc., Buffalo, New York (September 1965).
2. A. J. Landgrebe, An analytical method for predicting rotor wake geometry, J. American Helicopter Soc., 14, No. 4 (October 1969).
3. A. J. Landgrebe, An analytical and experimental investigation of helicopter rotor hover performance and wake geometry characteristics, USAAMRDL Technical Report 71-24, Eustis Directorate, US Army Air Mobility Research and Development Laboratory, Fort Eustis, Virginia (June 1971).
4. W. Johnson, A lifting surface solution for vortex induced airloads and its application to rotary wing airloads calculations, Massachusetts Institute of Technology, Aeroelastic and Structures Research Laboratory, TR 153-2 (April 1970).
5. J. D. Kocurek and J. L. Tangler, A prescribed wake lifting surface hover performance analysis, Presented at the 32nd Annual National Forum of the American Helicopter Soc., Preprint No. 1001 (May 1976).
6. J. M. Summa and D. R. Clark, A Lifting-surface method for hover/climb loads, Presented at the 35th Annual Forum of the American Helicopter Soc., Washington, D.C., Preprint No. 79-1 (May 1979).

7. F. X. Caradonna, The transonic flow on a helicopter rotor, Ph.D. Thesis, Stanford University (March 1978).
8. J. P. Rabbott Jr., Static-thrust measurements of the aerodynamic loading on a helicopter rotor blade, NACA TN 3688, Langley Aeronautical Laboratory, National Advisory Committee for Aeronautics, Langley Field, Virginia (February 1956).
9. J. Scheiman and H. L. Kelley, Comparison of flight-measured helicopter rotor-blade chordwise pressure distributions with static two-dimensional airfoil characteristics, NASA TN D-3936 (1967).
10. P. Brotherhood and C. Young, The measurement and interpretation of rotor blade pressures and loads on a puma helicopter in flight, Presented at the Fifth European Rotorcraft and Powered Lift Aircraft Forum, Amsterdam, The Netherlands (September 1979).
11. R. B. Gray, H. M. McMahon, K. R. Shenoy, and M. L. Hammer, Surface pressure measurements at two tips of a model helicopter rotor in hover, NASA CP-3281 (May 1980).
12. J. P. Sullivan, Experimental investigation of vortex rings and helicopter rotor wakes using a laser doppler velocimeter, D. S. Dissertation, Massachusetts Institute of Technology (June 1973).
13. J. D. Ballard, K. L. Orloff, and A. B. Luebs, Effect of tip shape on blade loading characteristics, Presented at the 35th Annual National Forum of the American Helicopter Soc., Washington, D.C., Preprint No. 79-1 (May 1979).
14. A. J. Landgrebe and B. V. Johnson, Measurements of model helicopter rotor flow velocities with a laser doppler velocimeter, Tech. Note, J. American Helicopter Soc., 19, No. 2 (July 1974).
15. D. W. Boatwright, Measurement of velocity component in the wake of a full scale helicopter rotor in hover, USAAMRDL TR 72-33 (August 1972).
16. C. V. Cook, The structure of rotor blade tip vortex, AGARD CP-111 (September 1972).
17. T. L. Holst, A fast, conservative algorithm for solving the transonic full-potential equation, AIAA Paper 79-1456 (July 1979).
18. S. C. Lee, Effect of turbulent boundary layer on transonic flows, Preliminary Report, NASA Interchange Number NCA2-OR450-001 (August 1979).



ROTOR BALANCING



BLADE CONSTRUCTION

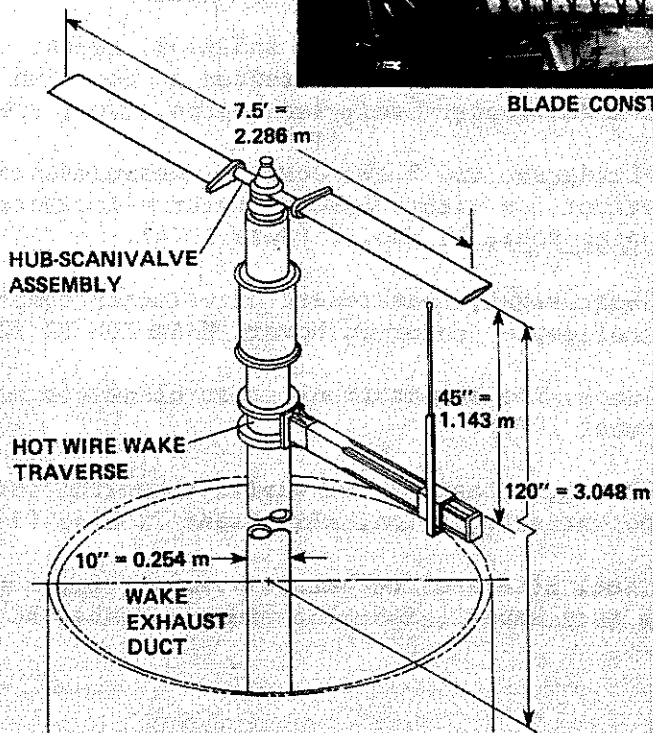


Fig. 1. The model and experimental set-up.

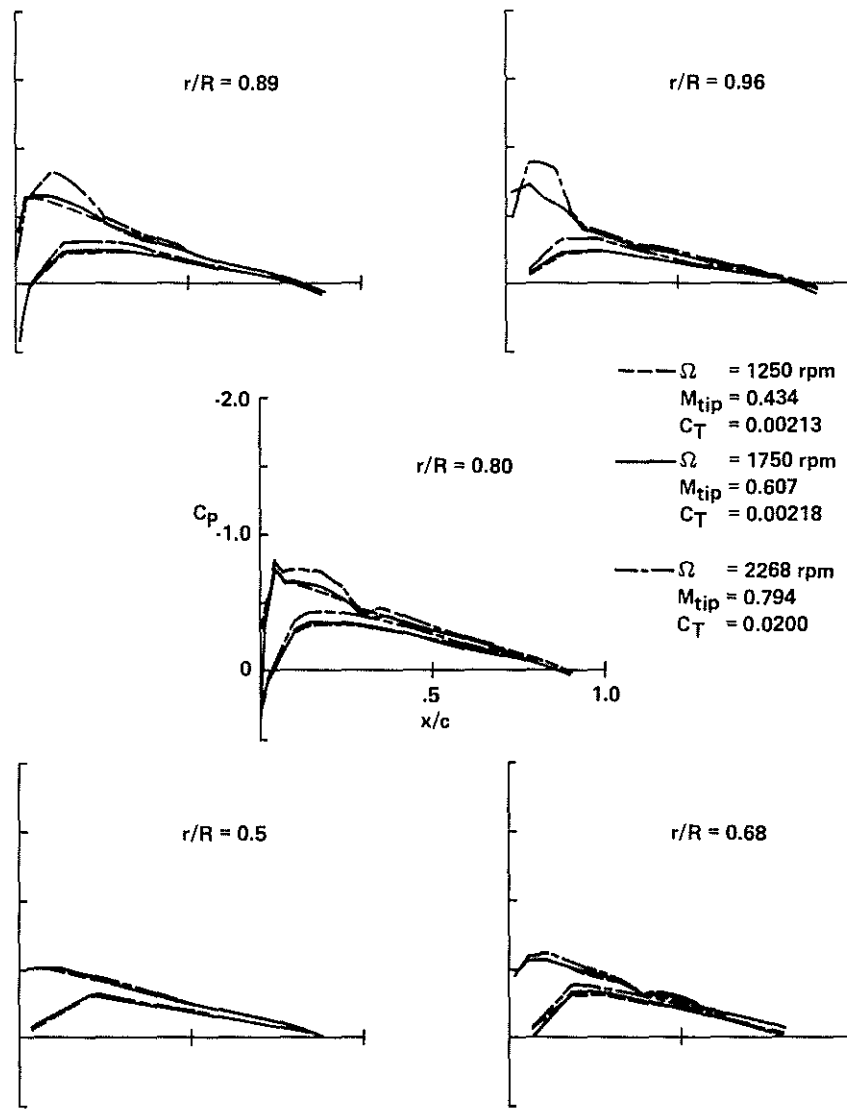


Fig. 2. Measured pressure distributions. Collective pitch, $\theta_c = 5^\circ$.

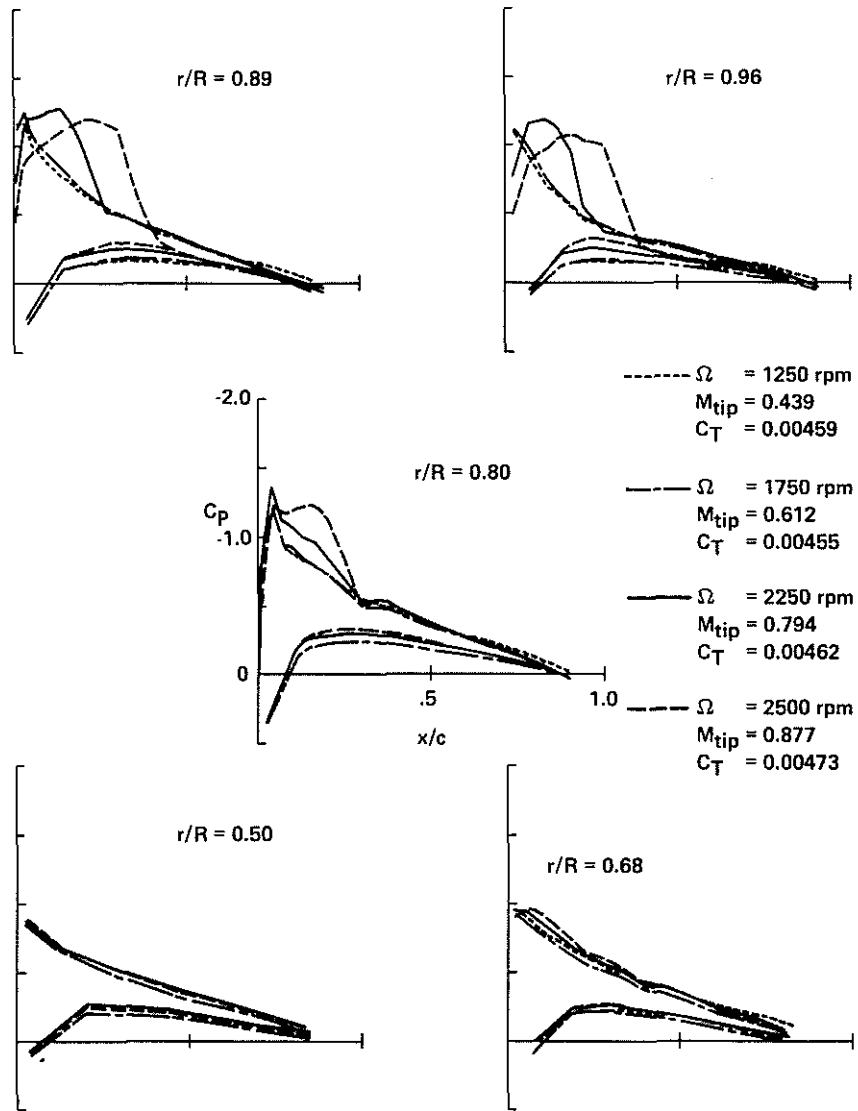


Fig. 3. Measured pressure distributions. Collective pitch, $\theta_c = 8^\circ$.

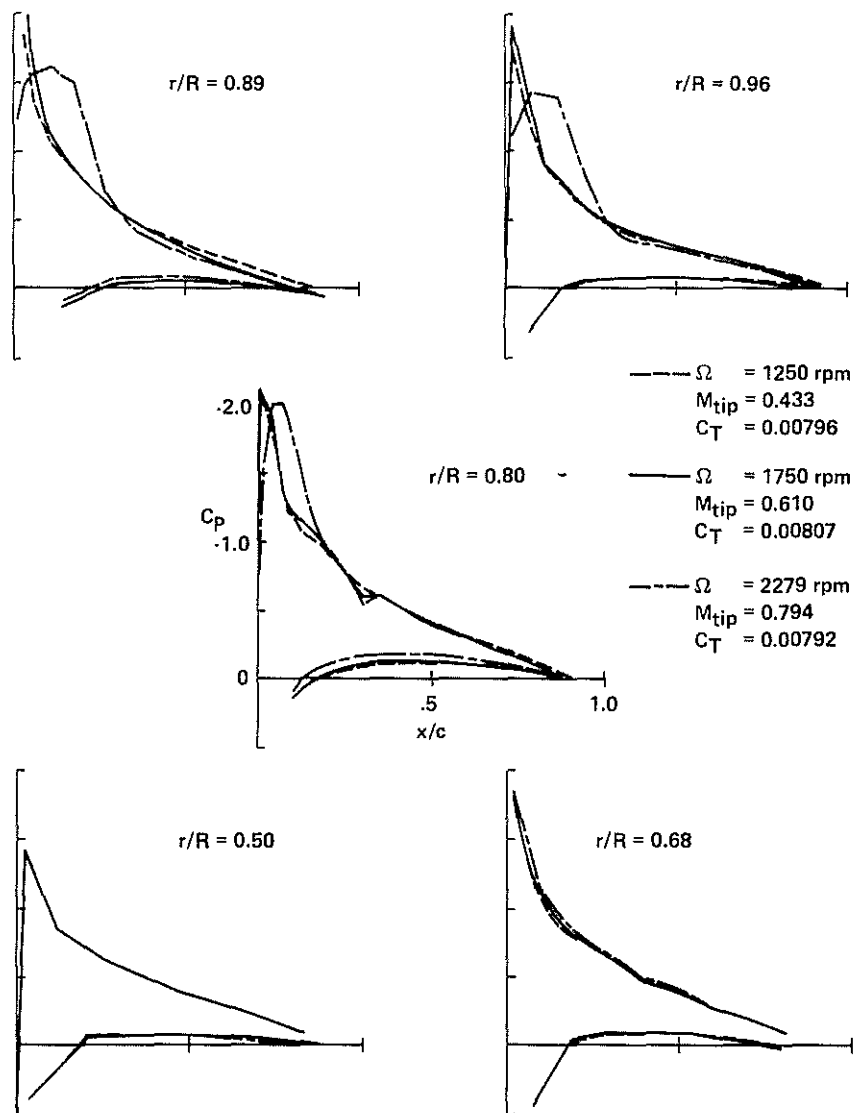


Fig. 4. Measured pressure distributions. Collective pitch, $\theta_c = 12^\circ$.

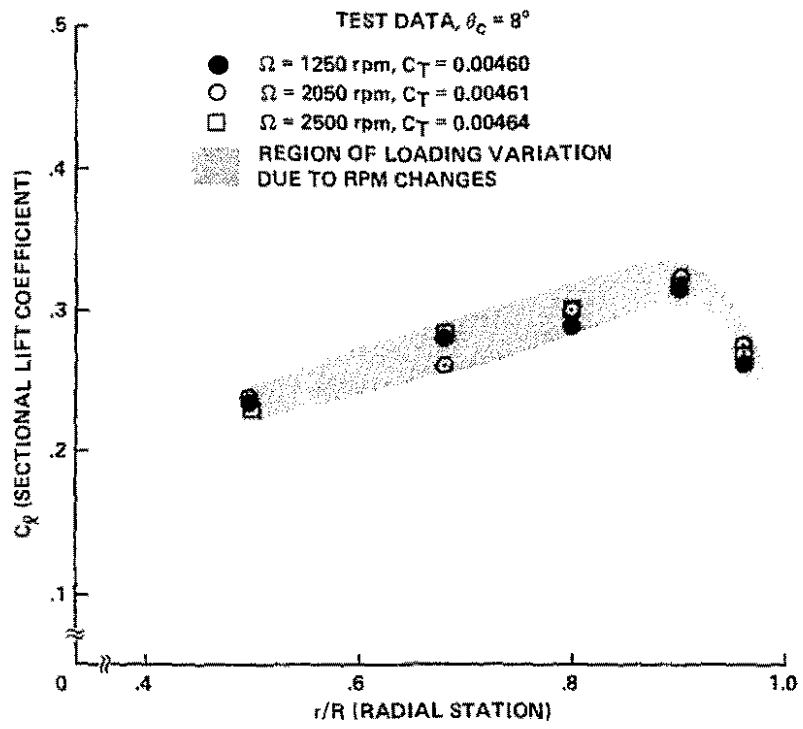


Fig. 5. Effect of rotor speed on blade span loading.

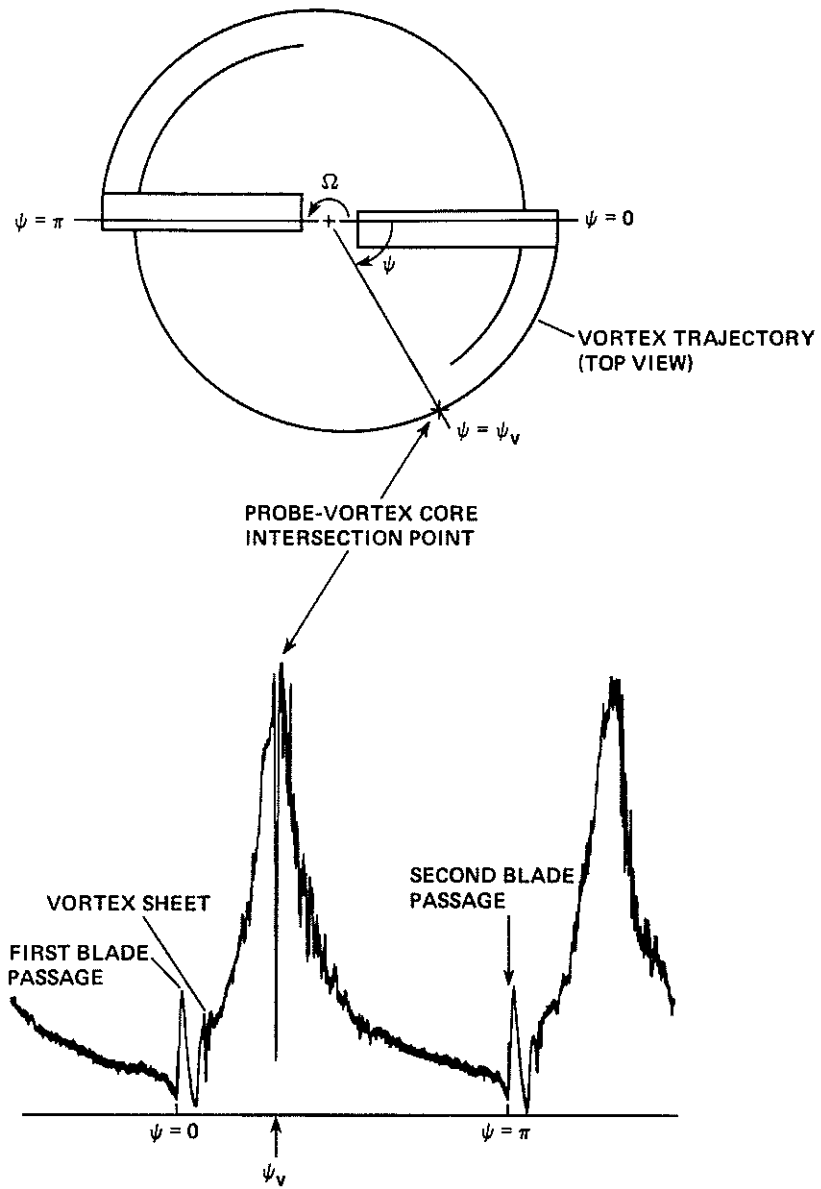


Fig. 6. Typical wake probe data.

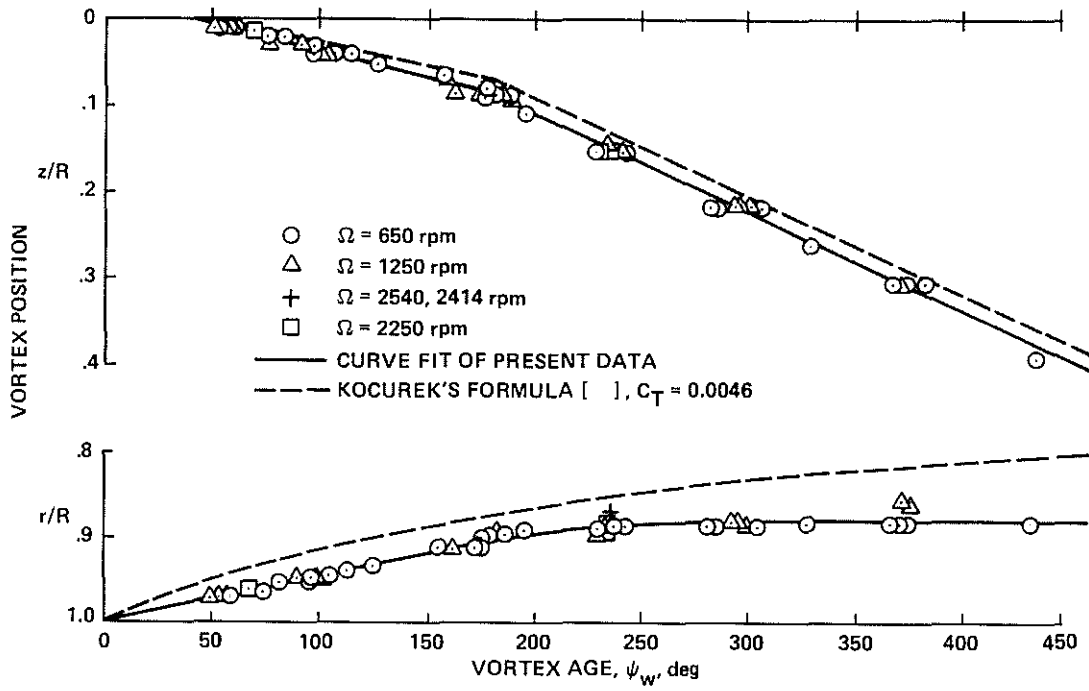


Fig. 7. Wake geometry measurements for various rotor speeds and comparison with classical data. Collective pitch, $\theta_c = 8^\circ$.

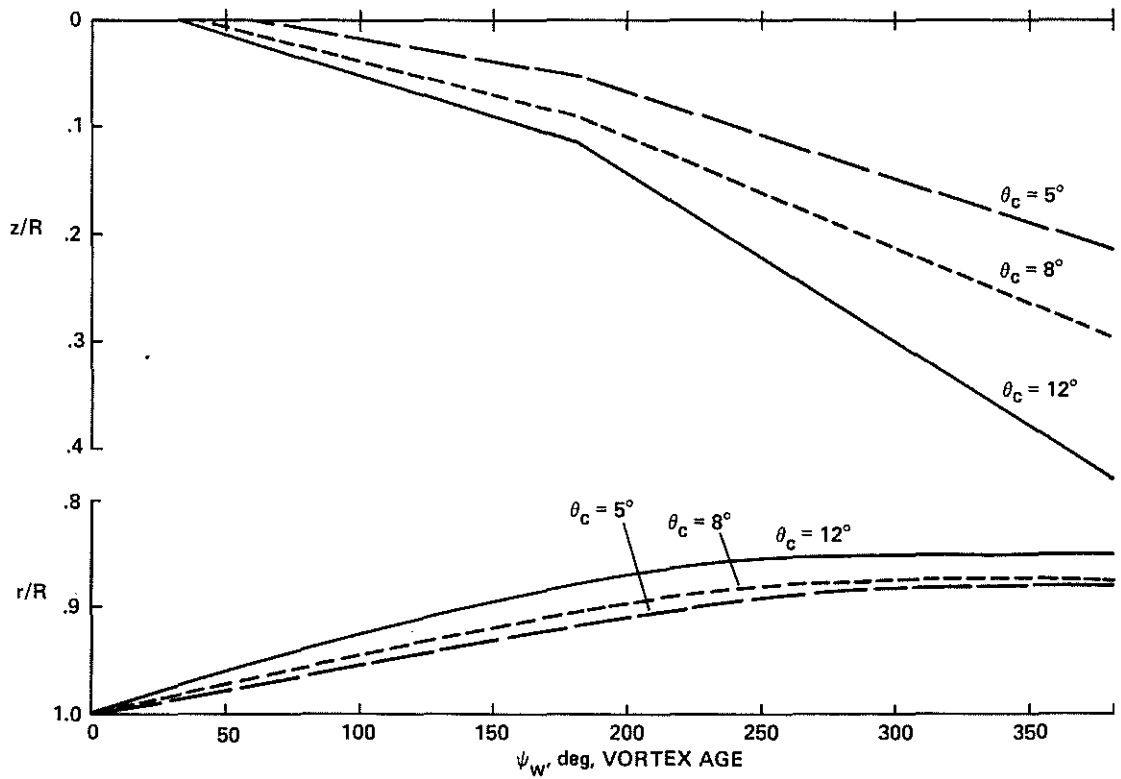


Fig. 8. Wake geometry for various pitch settings.

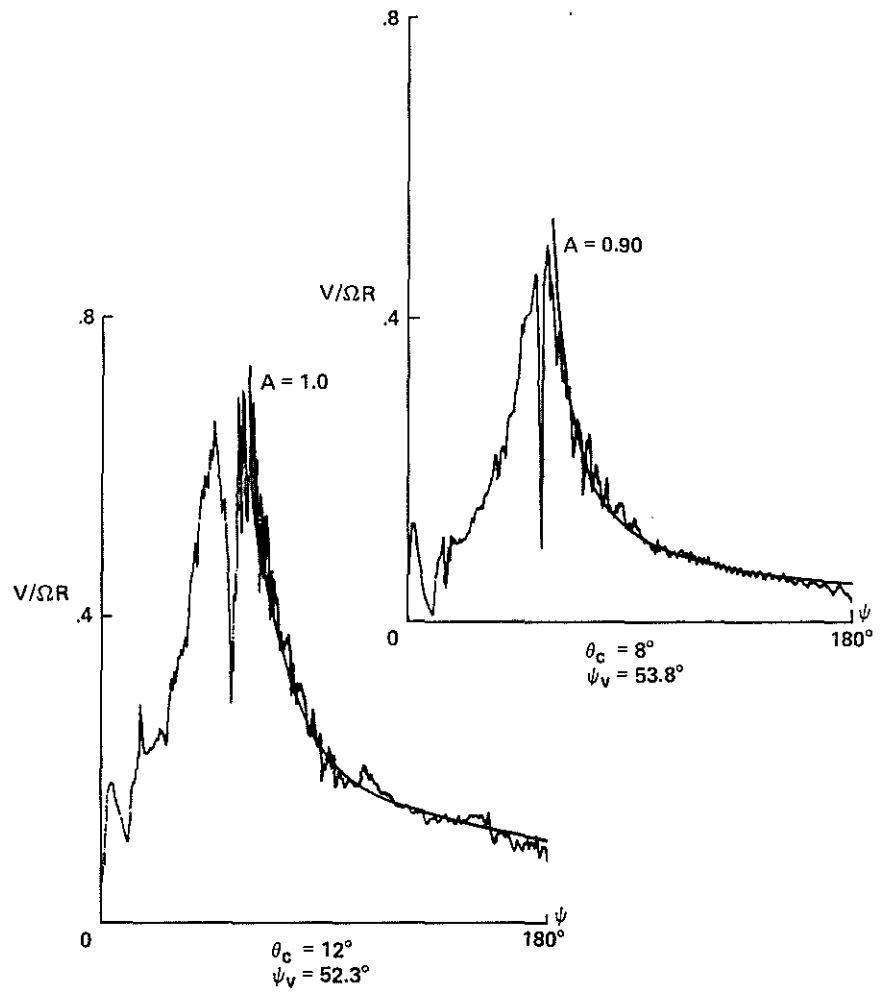


Fig. 9. Typical vortex velocity-time trace and 1/R curve fit for various pitch settings. Vortex age = 50° (nominal). $\Omega = 1250$ rpm.

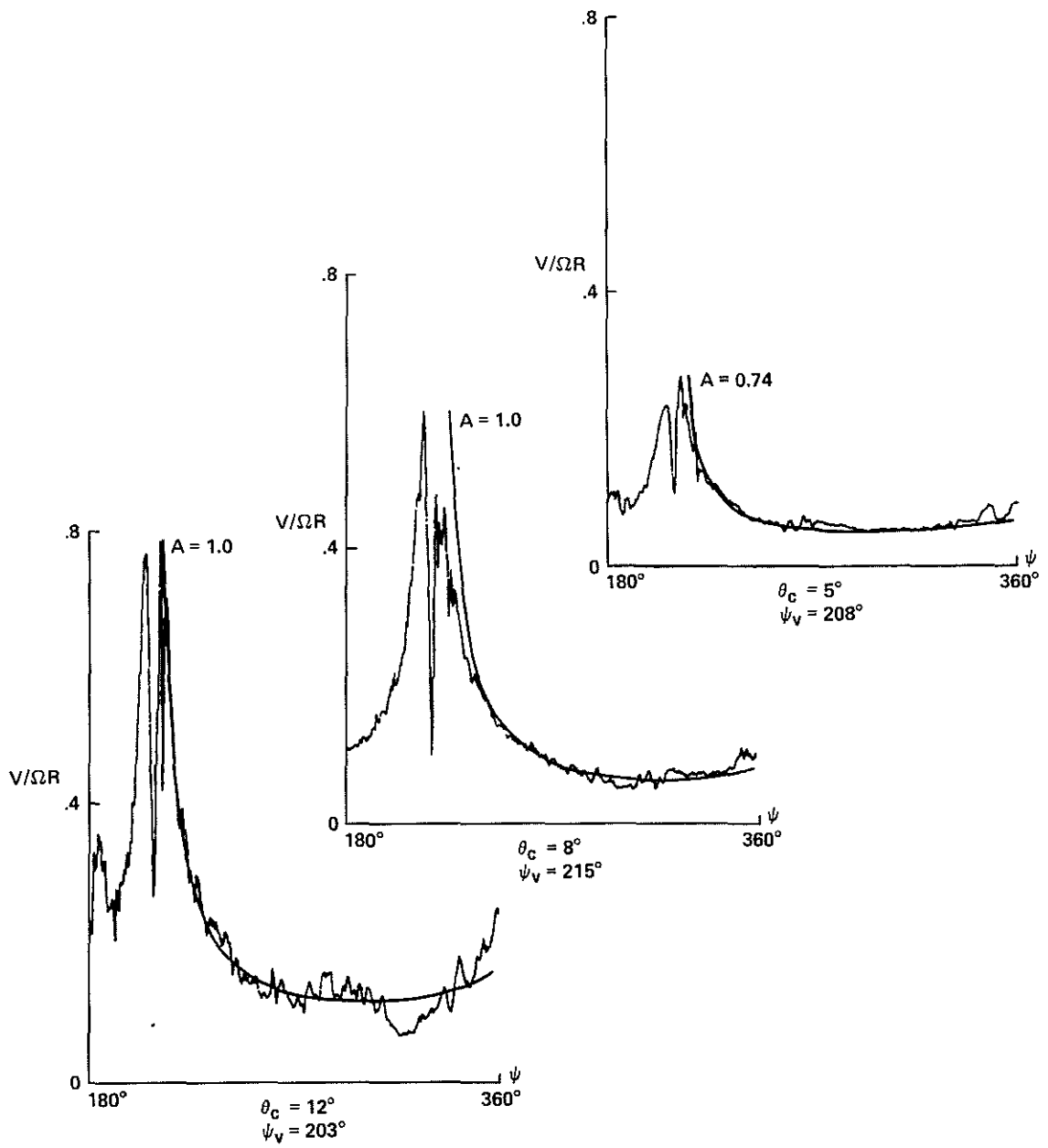


Fig. 10. Typical vortex velocity-time trace and $1/R$ curve fit for various pitch settings. Vortex age = 200° (nominal). $\Omega = 1250$ rpm.

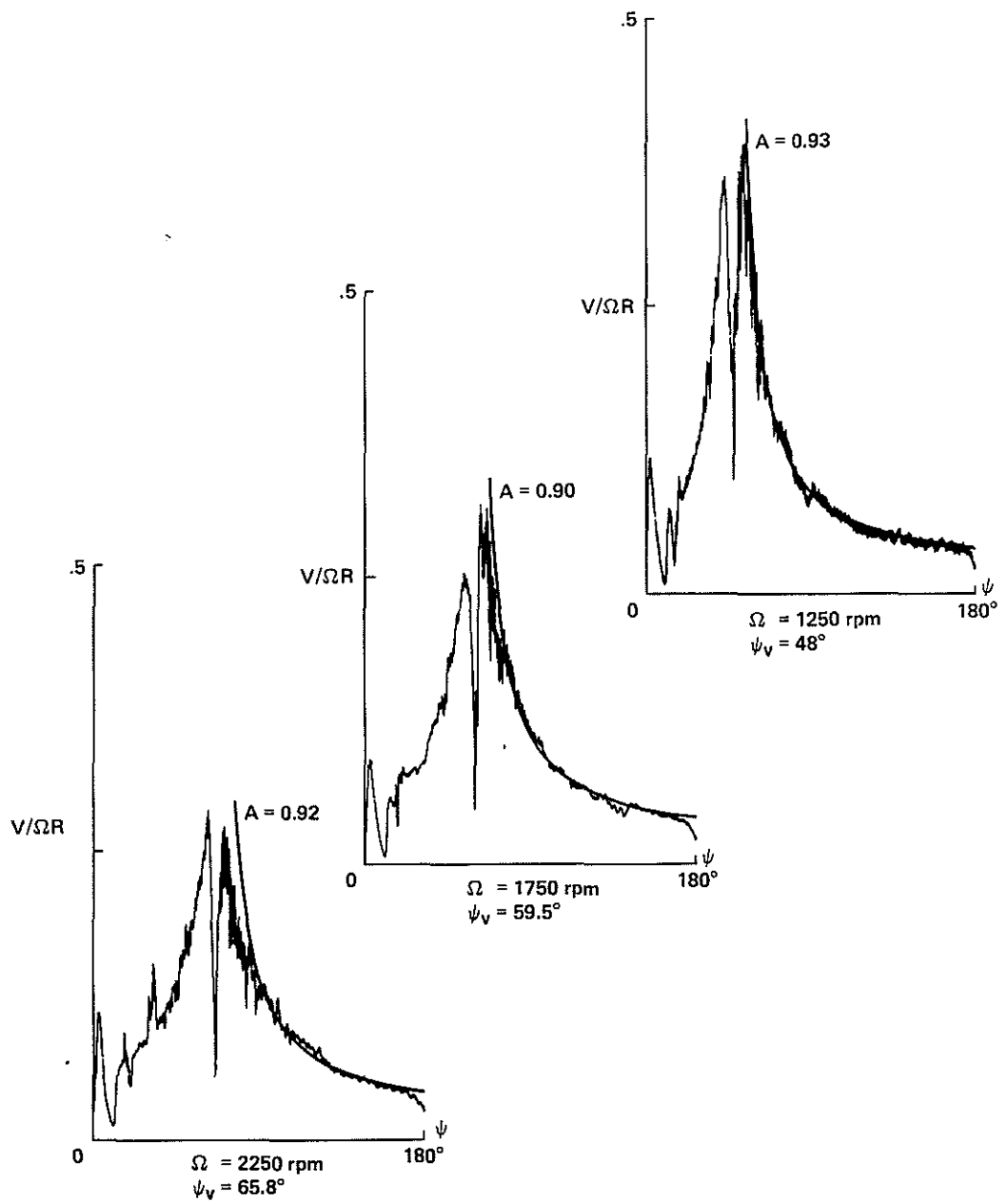


Fig. 11. Typical velocity-time trace and 1/R curve fit for various rotor speeds. Collective pitch, $\theta_c = 8^\circ$. Vortex age, $\psi_v \cong 50^\circ-65^\circ$.

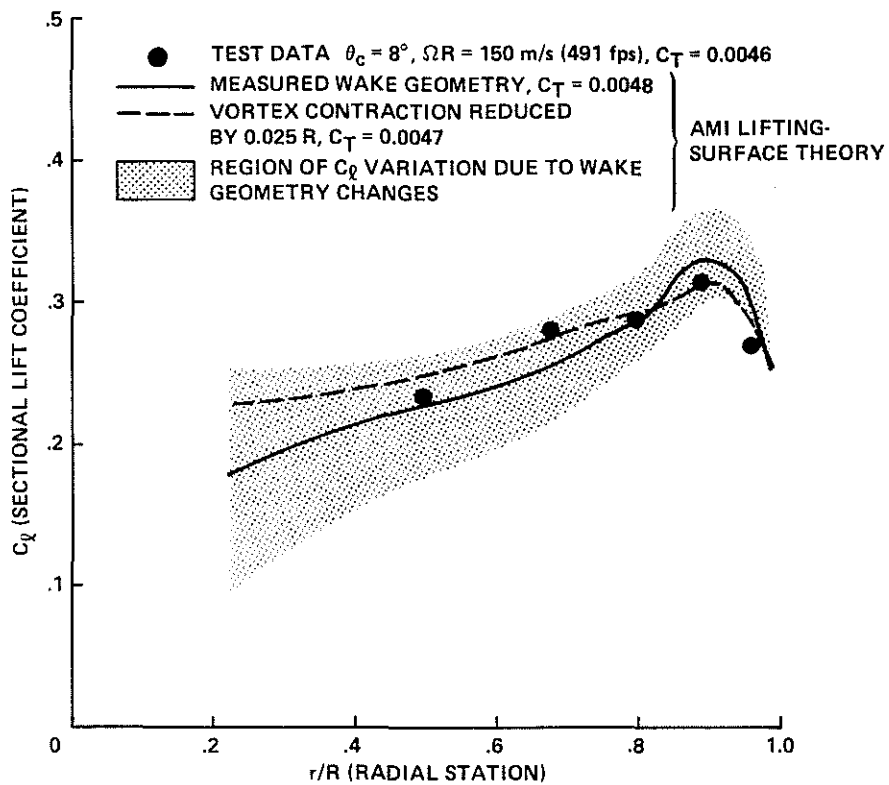


Fig. 12. Effect of vortex position on loading computation.

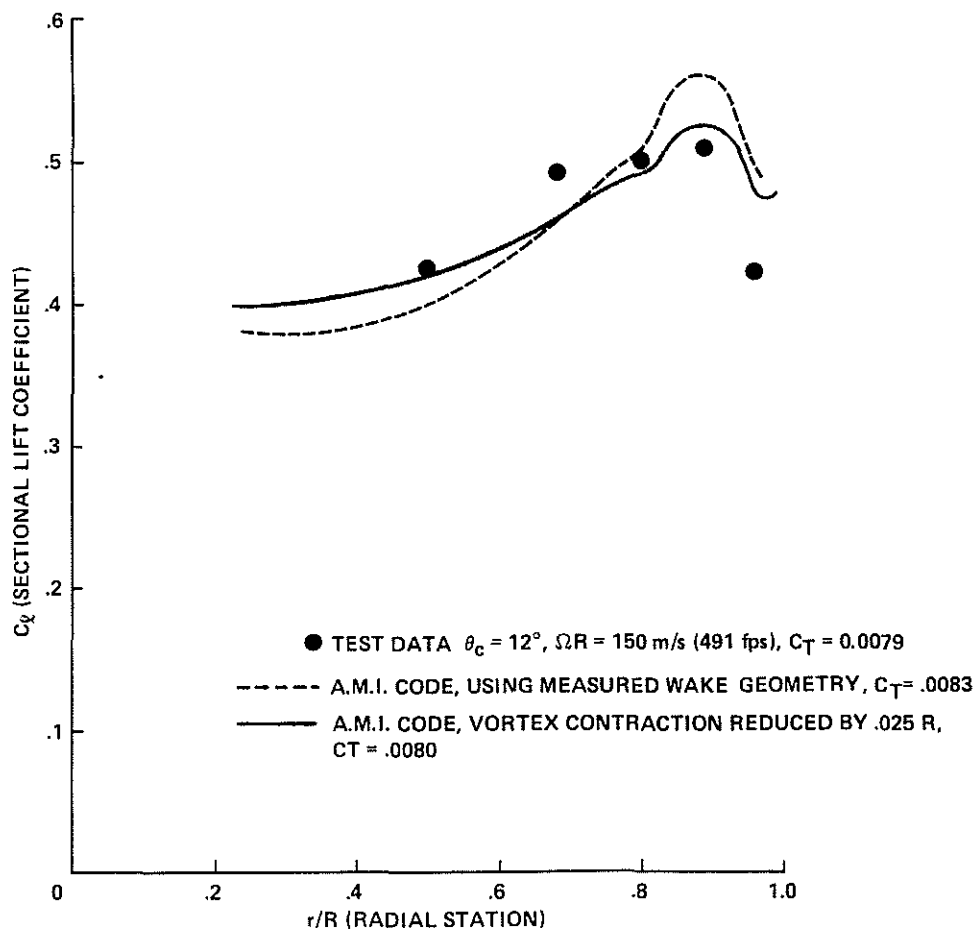


Fig. 13. Comparison of measured and computed loading.

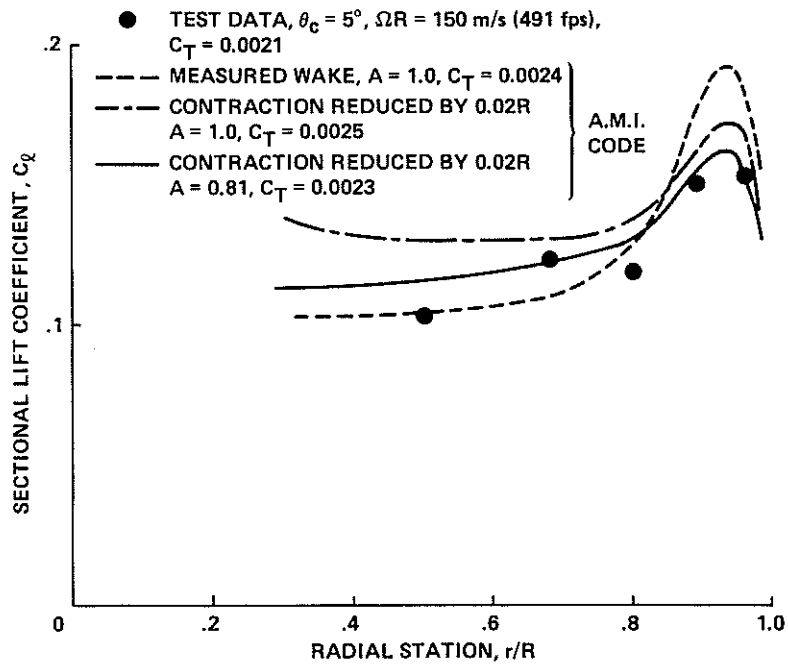


Fig. 14. Comparison of measured and computed loading.

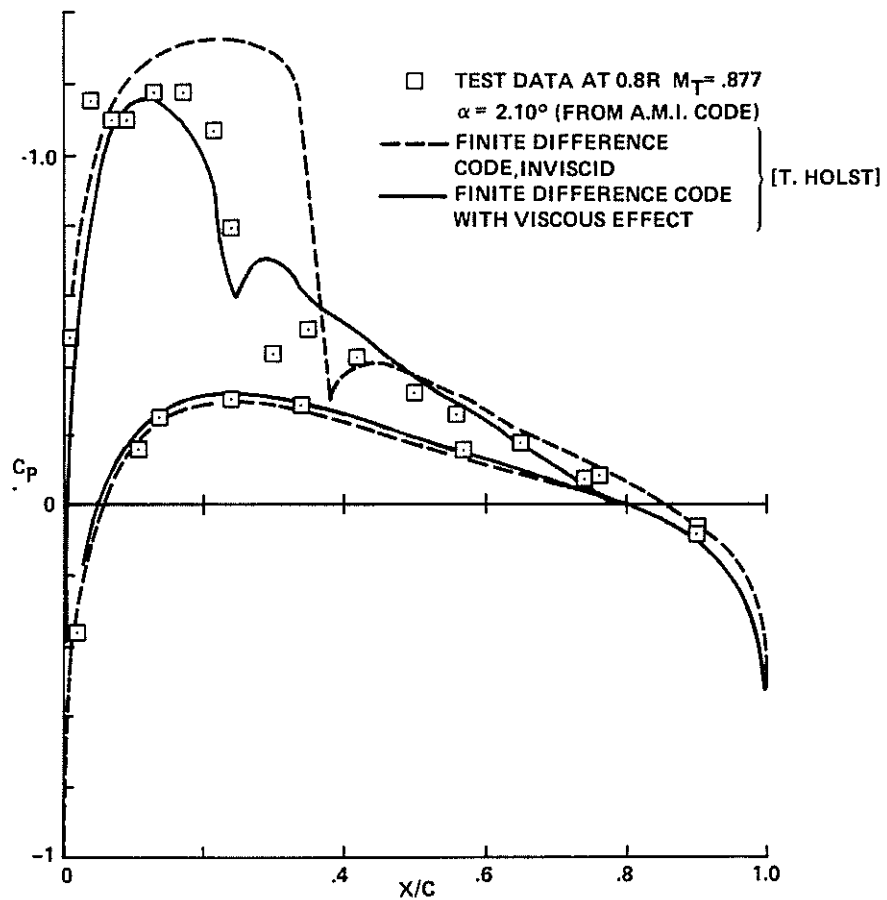


Fig. 15. Comparison of measured and computed chordwise pressure distribution.